

van der Waals force between a spherical tip and a solid surface

C. Girard

Laboratoire de Physique Moléculaire, Université de Franche-Comté, 25030 Besançon CEDEX, France

D. Van Labeke

Laboratoire d'Optique P. M. Duffieux, Université de Franche-Comté, 25030 Besançon CEDEX, France

J. M. Vigoureux

Laboratoire de Physique Moléculaire, Université de Franche-Comté, 25030 Besançon CEDEX, France

(Received 13 March 1989; revised manuscript received 20 July 1989)

We present a model for calculating the van der Waals interaction between a real surface and probe tip. The probe characterized by its dielectric constant is assumed locally spherical, and the description of the sample is based on a discrete atomic representation of the solid. This allows one to separate the van der Waals force into two different parts, which describe the continuum character and the corrugation of the surface, respectively. Numerical results corresponding to two different modes of imaging are proposed by varying two parameters: the radius of the probe and the distance of nearest approach. Finally, the model is used to discuss the structure sensitivity of the atomic force microscope on the (100) face of an ionic crystal.

I. INTRODUCTION

Force measurements between surfaces separated by a few nanometers are not new.¹ Indeed, for about twenty-five years it has been possible to measure directly the van der Waals forces between two planar surfaces. In these experiments the lateral facing areas were very large, and data have been tested from the macroscopic theories of Hamaker² and Lifshitz.^{3,4} These two methods ignore the atomic structure of real surfaces and describe the dynamic properties of the solids through a dielectric constant.

Very recently this field has generated renewed interest with the advent of atomic-force microscopy (AFM). Since the fundamental paper of Binnig, Quate, and Gerber,⁵ surface corrugations with a nanometric lateral resolution have been recorded by measuring the force between a thin tip and a surface.^{5,6} Similar resolutions have been reached on magnetic surfaces,⁷⁻⁹ and recently several groups have achieved atomic resolution. These authors have obtained AFM images of atomic corrugations on various surfaces (Gr, mica, . . .).¹⁰⁻¹²

In order to use the AFM, not only for the metrologic purposes, but also as a new physical probe to study surfaces, it is necessary to interpret this recent data. Such an interpretation, of course, needs to calculate the van der Waals force between the probe and the sample by going beyond the continuum approximation. As far as we know, little attention has been devoted to the calculation of the force between a tip and a surface described by a discrete model. In the case of tunneling microscopy, some studies have been reported of elastic strain deformations in the surface lattice when the tip is fully in contact.¹³⁻¹⁵ In the attractive mode a macroscopic Hamaker-type theory is used to simulate the interaction between a spherical tip and a flat surface.^{16,17} By con-

trast with these continuum approaches, we also find models where the tip-sample interaction is approximated by a Gordon-Kim (Ref. 12) potential between one atom of the tip and one atom of the surface.

The aim of this paper is to calculate the van der Waals force between the surface of a crystal and a probe tip. In recent AFM experiments this force is the only one in the attractive mode but remains important even in the repulsive mode. Thus, this allows us to examine how a given surface [the (100) face of NaCl or MgO] would appear when the probe is translated at a different distance from the surface and also to define the resolution with respect to the dimension of the probe and the nearest approach distance. For the sake of simplicity we consider here a spherical probe of radius a characterized by a local dielectric constant $\epsilon(\omega)$. This choice, which avoids complexity due to the conical shape of the probe used in the above experiments, nevertheless retains the main characters of the physical process. Such a model has been extensively used for calculating the current in scanning tunneling microscopy.¹⁸ In Sec. II we recall the expression of the dipolar dispersive energy between a sphere and an atom. This relation is applied in Sec. III to build the van der Waals potential through a pairwise summation between the probe and a face-centered-cubic crystal. In this way the van der Waals potential is expressed as a sum in the two-dimensional reciprocal lattice ($\mathbf{g} = m_1 \mathbf{g}_1 + m_2 \mathbf{g}_2$) associated with each plane p parallel to the surface of the crystal. Such a method has been proposed by Steele¹⁹ and was used to study various physisorption phenomena on corrugated surfaces.²⁰⁻²⁸ This procedure allows us to separate the van der Waals force in two different contributions. The first-one, corresponding to the term for which $\mathbf{g} = 0$, represents the continuum part of the interaction. This term does not depend on the lateral position of the probe and represents the main contribution of the at-

tractive force. The second one, corresponding to the terms with $g \neq 0$, characterizes the corrugation experienced by the probe. It is consequently the term which contains the information on the atomic structure of the sample. In Sec. IV the van der Waals force is derived from the interaction energy and is discussed. Numerical results are presented in two different modes of imaging: the constant tip-height mode and the constant force mode.

II. THE ATOM-SPHERE INTERACTION

The dispersive energy between a point particle (atom or molecule) and a dielectric sphere may be determined in the framework of the coupled modes method.²⁹⁻³¹ In a recent contribution, Marvin and Toigo (Ref. 31) have elaborated a very general formalism based on this method, allowing the calculation of this energy between an atom and another system of arbitrary shape. In the particular case of the sphere of radius a and in the electrostatic limit, one has

$$E(\mathbf{R}) = -\frac{\hbar a}{\pi R^4} \int_0^{+\infty} \alpha(i\xi) \sum_{n=0}^{\infty} L_n(i\xi) [\epsilon(i\xi) - 1] \times \left[\frac{a}{R} \right]^{2n} \frac{n(n+1)}{2} d\xi, \quad (1)$$

where $\epsilon(\omega)$ and $\alpha(\omega)$ represent the dielectric constant of the sphere and the dipolar polarizability of the atom, respectively; R labels the distance between the nucleus of the atom and the center of the sphere. Moreover in Eq. (1), $L_n(\omega)$ defines the screening factor appearing after application of the boundary conditions at the surface of the sphere:

$$L_n(\omega) = \frac{2n+1}{n\epsilon(\omega) + n + 1}. \quad (2)$$

Note that in a nonlocal approach, where the dispersion spatial effects are included in the dynamic treatment of the response properties of the sphere, this factor may be expressed by a more general form:³²

$$L_n^{\text{NL}}(\omega) = \frac{(2n+1)a}{(n+1)F_n(a, \omega) + a}, \quad (3)$$

where we define, following Dasgupta and Fuchs,³³

$$F_n(r, \omega) = \frac{2}{\pi} \int_0^{+\infty} [j_n(kr)j_n(ka) / \epsilon(\mathbf{k}, \omega)] dk. \quad (4)$$

In this expression, $\epsilon(k, \omega)$ is the nonlocal bulk dielectric constant of the sphere and $j_n(kr)$ is the spherical Bessel function.

III. INTERACTION BETWEEN A DIELECTRIC SPHERE AND A DISCRETE SOLID

As was originally done by Hamaker² for the attraction energy between two solids, one may, in our problem, consider that the van der Waals energy is the sum of all the

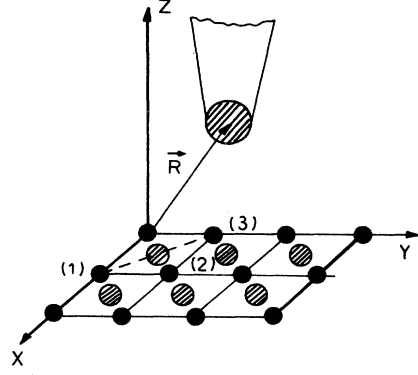


FIG. 1. Geometry of the tip and the NaCl(100) surface. $\mathbf{R} = (x, y, d)$ characterizes the position of the center of the sphere used to represent the probe. Solid and dashed circles represent the ions Na^+ and Cl^- , respectively.

pairs energy including the sphere and each of the atoms belonging to the solid. Thus, in a first approximation, when one neglects the possible many-body contributions connected to the interaction between several atoms belonging to the crystal and sphere, we can write the interaction energy as

$$E_{\text{vdW}}(\mathbf{R}) = \sum_{n_1, n_2} \sum_{s, p} E(\mathbf{R} - \mathbf{r}_{n_1, n_2, s, p}), \quad (5)$$

where \mathbf{R} labels the position vector of the probe (Fig. 1):

$$\mathbf{R} = (l, d) \equiv (x, y, d) \quad (d > 0) \quad (6)$$

and where $\mathbf{r}_{n_1, n_2, s, p}$ is given by

$$\mathbf{r}_{n_1, n_2, s, p} = n_1 \mathbf{a}_1 + n_2 \mathbf{a}_2 - pb \mathbf{u}_z + \boldsymbol{\tau}_{s, p}, \quad (7)$$

where the subscripts n_1 and n_2 characterize the location of a given primitive cell belonging to the p th plane parallel to the surface of the solid.²⁴ Moreover \mathbf{a}_1 and \mathbf{a}_2 represent the lattice vectors in a given plane p , b labels the interplanar distance, \mathbf{u}_z defines the unit vector perpendicular to the surface, and s labels a given atom of the primitive cell. In a case of a fcc crystal the vector $\boldsymbol{\tau}_{s, p}$ is given by

$$\boldsymbol{\tau}_{s, p} = \frac{1}{4}(\mathbf{a}_1 + \mathbf{a}_2)[1 - (-1)^{s+p}]. \quad (8)$$

Let us write Eq. (5) as a spatial integral on the whole solid. It then becomes

$$E_{\text{vdW}}(\mathbf{R}) = \int dl dz_1 E(\mathbf{r}_1 - \mathbf{R}) \times \sum_{s, p} \delta(z_1 - z_p) \times \sum_{n_1, n_2} \delta(l_1 - n_1 \mathbf{a}_1 - n_2 \mathbf{a}_2 - \boldsymbol{\tau}_{s, p}). \quad (9)$$

The periodic arrangement of the atoms in the solid is characterized by the vector $n_1 \mathbf{a}_1 + n_2 \mathbf{a}_2$. This allows us to expand the function $\sum_{n_1, n_2} \delta(l_1)$ in the reciprocal lattice ($\mathbf{g} = m_1 \mathbf{g}_1 + m_2 \mathbf{g}_2$). One has then

$$\sum_{n_1, n_2} \delta(l_1 - n_1 a_1 - n_2 a_2 - \tau_{s,p}) = \frac{1}{S} \sum_{\mathbf{g}} \exp[i\mathbf{g} \cdot (l_1 - \tau_{s,p})], \quad (10)$$

where S represents the area of the primitive cell. By taking into account this expression one may write

$$E_{\text{vdW}}(\mathbf{R}) = \frac{1}{S} \sum_{s,p} \sum_{\mathbf{g}} \exp(-i\mathbf{g} \cdot \tau_{s,p}) \times \int dl_1 E((l_1, z_p) - \mathbf{R}) \exp(i\mathbf{g} \cdot l_1) \quad (11)$$

when replacing the Eq. (1) into this relation, the interaction energy may be rewritten as

$$E_{\text{vdW}}(\mathbf{R}) = -\frac{\hbar}{\pi S} \sum_{n=0}^{\infty} \frac{n(n+1)}{2} a^{2n+1} \sum_{s,p} C_{s,n} \sum_{\mathbf{g}} \exp[-i\mathbf{g} \cdot (l_1 + \tau_{s,p})] \int dl_1 \frac{\exp(i\mathbf{g} \cdot l_1)}{[l_1^2 + (pb+d)^2]^{n+2}} \quad (12)$$

in which the factor $C_{s,n}$ defines the n th strength coefficient between the probe and an atom (s) of the solid. It is given by

$$C_{s,n} = \int_0^{+\infty} \alpha_s(i\xi) [\epsilon(i\xi) - 1] L_n(i\xi) d\xi. \quad (13)$$

Equation (12) may be separated in two different contributions:

$$E_{\text{vdW}}(\mathbf{R}) = \bar{E}_{\text{vdW}}(l, d) + \tilde{E}_{\text{vdW}}(l, d), \quad (14)$$

where $\bar{E}_{\text{vdW}}(d)$ represents the continuum part, obtained by putting $\mathbf{g}=0$ in Eq. (12), of the attractive energy. After integrating this term on l_1 we have

$$\bar{E}_{\text{vdW}}(d) = -\frac{\hbar}{S} \sum_{n=0}^{\infty} \frac{1}{2} \sum_{s,p} C_{s,n} \frac{1}{(d+pb)^{2(n+1)}}. \quad (15)$$

The second part $\tilde{E}_{\text{vdW}}(l, d)$ characterizes the corrugation energy of the system probe surface. This quantity, which depends on the lateral displacement l of the sphere, appears as a sum in the reciprocal lattice of various spatial harmonics which takes into account the discrete nature of the surface. We have

$$\tilde{E}_{\text{vdW}}(l, d) = -\frac{2\hbar}{S} \sum_{n=0}^{+\infty} n(n+1) a^{2n+1} \sum_{s,p} C_{s,n} \sum_{\substack{m_1 > 0 \\ m_2 \neq 0}} \cos[\mathbf{g} \cdot (l + \tau_{s,p})] \int_0^{\infty} dl_1 l_1 J_0(gl_1) \frac{1}{[l_1^2 + (d+pb)^2]^{n+2}}, \quad (16)$$

where J_0 represents a Bessel function. Now, in order to perform the integral on l_1 , we can use the following identity:¹⁹

$$\int_0^{+\infty} J_0(gl_1) (l_1^2 + Z^2)^{-n} l_1 dl_1 = \frac{1}{(n-1)!} \left(\frac{g}{2Z} \right)^{n-1} K_{n-1}(gZ) \quad (17)$$

in which K_n labels the corresponding modified Bessel function. Equation (16) then becomes

$$\tilde{E}_{\text{vdW}}(l, d) = -\frac{2\hbar}{S} \sum_{n=0}^{+\infty} \left[\frac{1}{(n-1)!} a^{2n+1} \sum_{s,p} C_{s,n} \sum_{\substack{m_1 > 0 \\ m_2 \neq 0}} \cos[\mathbf{g} \cdot (l + \tau_{s,p})] \left(\frac{g}{2(d+pb)} \right)^{n+1} K_{n+1}(g(d+pb)) \right]. \quad (18)$$

Some remarks may be done about these results [Eqs. (15) and (16)].

(i) When the sphere reduces to a single atom of dynamic polarizability $\alpha_a(\omega)$, the $C_{s,n}$ strength coefficient becomes

$$C_{s,n} = \int_0^{+\infty} \alpha_a(i\xi) \alpha_s(i\xi) d\xi \quad (19)$$

and Steele's result is then recovered.¹⁹

(ii) Due to the presence in Eq. (18) of the Bessel functions $K_{n+1}(g(d+pb))$, the corrugation energy decreases very strongly with respect to the distance d between the center of the sphere and the surface. By contrast, in the continuum part of the van der Waals energy, the d depen-

dence is more smooth. Consequently, the corrugation of a surface appears in AFM as a very sensitive quantity to the approach distance of the probe. More details about these points will be given in the following section.

(iii) The magnitude of the van der Waals energy depends on the numerical value of the strength coefficient $C_{s,n}$ [Eq. (13)]. In the particular approximation when one chooses all screening factors $L_n(\omega)$ identical to those for which $n=1$, one has

$$C_{s,n} = 3 \int_0^{+\infty} \left[\frac{\epsilon(i\xi) - 1}{\epsilon(i\xi) + 2} \right] \alpha_s(i, \xi) d\xi. \quad (20)$$

In this case Eqs. (15) and (16) take a simplified form:

$$\bar{E}_{\text{vdW}}(d) = -\frac{3\hbar}{4S} \sum_s \left[\int_0^{+\infty} \alpha_s(i, \xi) \left[\frac{\epsilon(i\xi) - 1}{\epsilon(i\xi) + 2} \right] d\xi \right] \sum_p \frac{8\pi a^3}{[(d+pb)^2 - a^2]^2} \quad (21)$$

and

$$\bar{E}_{\text{vdW}}(l, d) = -\frac{3\hbar}{4S} \sum_s \left[\int_0^{+\infty} \alpha_s(i\xi) \left[\frac{\epsilon(i\xi) - 1}{\epsilon(i\xi) + 2} \right] d\xi \right] \sum_p \sum_{\substack{m_1 > 0 \\ m_2 \neq 0}} \cos[\mathbf{g} \cdot (l + \tau_{s,p})] \frac{8\pi a^3 g^2}{[(d+pb)^2 - a^2]} K_2(g[(d+pb) - a^2]^{1/2}). \quad (22)$$

Thus, this approximation eliminates the summation over the index n and allows a more simple numerical study.

IV. NUMERICAL APPLICATIONS

In this section we present numerical calculations based on the relations (21) and (22) for a tungsten sphere interacting with the (100) face of a fcc crystal (NaCl, MgO, ...). We first define some auxiliary functions which allow one to calculate the factor defined as

$$C_{as} = \frac{3\hbar}{4} \int_0^{+\infty} \alpha_s(i\xi) \left[\frac{\epsilon(i\xi) - 1}{\epsilon(i\xi) + 2} \right] d\xi. \quad (23)$$

The polarizability $\alpha_s(i\xi)$ is a monotonically decreasing function of ξ , starting from the static polarizability $\alpha_s(0)$ and falling off as ξ^{-2} in the limit $\xi \rightarrow \infty$. A useful approximation to this function is given by the simple Drude model,

$$\alpha_s(i\xi) = \frac{\alpha_s(0)\omega_s^2}{\xi^2 + \omega_s^2}, \quad (24)$$

where $\alpha_s(0)$ represents the static polarizability in crystal and ω_s an effective frequency obtained from the C_6 dispersion coefficient between two atoms of the solid:

$$C_6 = \frac{3}{4} \alpha_s^2(0) \omega_s. \quad (25)$$

Moreover, in the case of a metallic sphere, $\epsilon(i\xi)$ may be written

$$\epsilon(i\xi) = 1 + \frac{\omega_p^2}{\xi^2}, \quad (26)$$

where ω_p is the plasma frequency of the conductor. Then the coefficient C_{as} becomes

$$C_{as} = \frac{\sqrt{3}\omega_s\omega_p\alpha_s(0)}{32(\omega_s + \omega_p/\sqrt{3})}. \quad (27)$$

Numerical values of C_{as} are given in Table I for several surfaces.

A. The van der Waals force between the probe and the surface

The normal component of the force between the probe and the solid can be deduced from Eqs. (21) and (22). This yields

$$F(l, d) = \bar{F}(l, d) + \bar{F}(l, d) \quad (28)$$

with

$$\bar{F}(d) = -\frac{8\pi a^3}{S} \sum_s C_{as} \sum_p \frac{4(d+pb)}{[(d+pb)^2 - a^2]^3} \quad (29)$$

and

$$\bar{F}(l, d) = -\frac{8\pi a^3}{S} \sum_s C_{as} \sum_p \sum_{\substack{m_1 > 0 \\ m_2 \neq 0}} \cos[\mathbf{g} \cdot (l + \tau_{s,p})] \frac{g^3(d+pb)}{[(d+pb)^2 - a^2]^{3/2}} K_3(g[(d+pb) - a^2]^{1/2}). \quad (30)$$

Note that in Eqs. (29) and (30) in order to obtain a correct convergence we have to take into account ten atomic planes in the summation on p . This means that the force between the tip and the surface is also sensitive to the presence of the atoms belonging to planes $p \neq 0$. Moreover, in the asymptotic limit when the planes are infinitely close it is then possible to replace the sum over p by an integral:³⁴

$$\sum_p \rightarrow \frac{1}{b} \int_0^{-\infty} dz. \quad (31)$$

One recovers then the macroscopic Hamaker result² giving the force between a plane and a spherical tip:

$$F(d) = -\frac{Aa}{d-a}. \quad (32)$$

This formula has been proposed in Refs. 16 and 17 to estimate the van der Waals attractive force. However, it is important to remark that for short distance d , the two relations (28) and (32) give very different numerical results and rigorous predictions in AFM should be performed from the discrete approach described in this paper.

TABLE I. The constants used to define the C_{as} coefficient (a.u.) between an atom of the surface and a tungsten probe ($\omega_p = 0.844$).

Atom	$\alpha_s(0)^a$	ω_s	C_{as}
Na	1.002	2.108	0.036
Cl	21.153	0.475	0.481
Mg	0.486	3.025	0.019
O	12.32	0.531	0.293

^aReference 35.

TABLE II. Structure parameters for the (100) face of NaCl and MgO (a.u.).

	Constant			
	a_1	τ_{10}	b	g_1
NaCl	7.54	3.77	5.33	0.833
MgO	5.63	2.81	3.98	1.116

TABLE III. The van der Waals attractive force between a tip of radius $a=2 \text{ \AA}$ and a (100) face of NaCl. The probe follows the path (1)–(3) (cf. Fig. 1) and the distance of nearest approach $\bar{d}=2.5 \text{ \AA}$.

$X=Y (\text{\AA})^a$	$\bar{F}(l,d)$ (10^{-10} N)	$F(l,d)$ (10^{-10} N)
0	0.254	-1.59
$a_1/10$	0.215	-1.63
$2a_1/10$	0.092	-1.75
$3a_1/10$	-0.098	-1.94
$4a_1/10$	-0.284	-2.13
$5a_1/10$	-0.363	-2.21

^a $a_1 = 3.99 \text{ \AA}$.

TABLE IV. The van der Waals attractive force between a tip of radius $a=2 \text{ \AA}$ and a (100) face of NaCl. The probe follows the path (1)–(2) and the distance of nearest approach $\bar{d}=2.5 \text{ \AA}$.

$X (\text{\AA})^a$	$\bar{F}(l,d)$ (10^{-10} N)	$F(l,d)$ (10^{-10} N)
0	0.261	-1.62
$a_1/10$	0.242	-1.65
$2a_1/10$	0.191	-1.69
$3a_1/10$	0.126	-1.76
$4a_1/10$	0.071	-1.81
$5a_1/10$	0.050	-1.83

^a $a_1 = 3.99 \text{ \AA}$.

TABLE V. Same caption as Table III, but for a (100) face of MgO.

$X=Y (\text{\AA})^a$	$\bar{F}(l,d)$	$F(l,d)$
0	0.067	-2.09
$a_1/10$	0.055	-2.11
$2a_1/10$	0.022	-2.14
$3a_1/10$	-0.029	-2.19
$4a_1/10$	-0.062	-2.23
$5a_1/10$	-0.078	-2.24

^a $a_1 = 2.98 \text{ \AA}$.

TABLE VI. Same caption as Table IV, but for a (100) face of MgO.

$X=Y (\text{\AA})^a$	$\bar{F}(l,d)$	$F(l,d)$
0	0.067	-2.09
$a_1/10$	0.061	-2.10
$2a_1/10$	0.045	-2.12
$3a_1/10$	0.026	-2.14
$4a_1/10$	0.010	-2.15
$5a_1/10$	0.005	-2.16

^a $a_1 = 2.98 \text{ \AA}$.

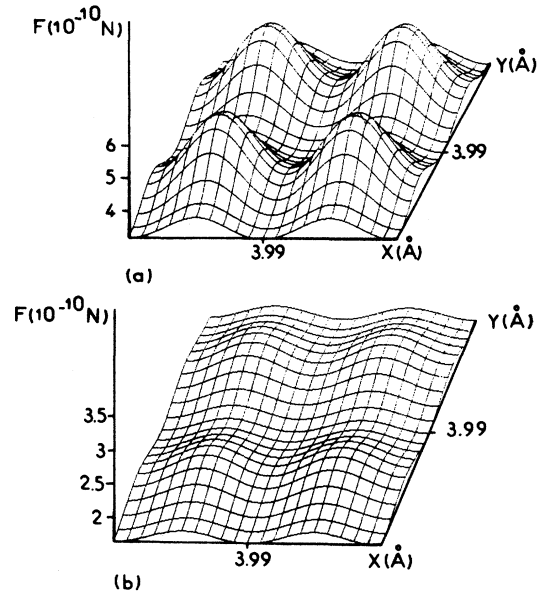


FIG. 2. Attractive van der Waals force (in N) between a spherical probe of radius $a=2 \text{ \AA}$ and a (100) face of a crystal NaCl: (a) $\bar{d}=d-a=2 \text{ \AA}$; (b) $\bar{d}=d-a=2.5 \text{ \AA}$.

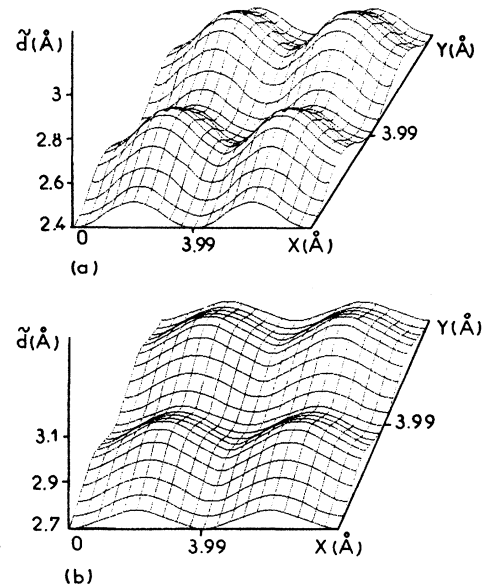


FIG. 3. The tip height \bar{d} (in \AA) calculated for two values of the van der Waals force and of the radius of the probe: (a) $F=1.8 \times 10^{-10} \text{ N}$ and $a=2 \text{ \AA}$, (b) $F=3.8 \times 10^{-10} \text{ N}$ and $a=2.5 \text{ \AA}$.

The numerical data needed to calculate $\bar{F}(l, d)$ and $\bar{F}(l, d)$ are gathered in Tables I and II. Numerical results are presented for NaCl and MgO in Tables III–VI and in Figs. 2–4 for the (100) face of NaCl. Several remarks may be made about these results.

(i) The total force $F(d, l)$ is always negative in the frame of Fig. 1. This feature corresponds to the attractive character of van der Waals force. The numerical magnitude order of $F(d, l)$ varies between 10^{-10} and 10^{-11} N which is measurable in the AFM.

(ii) It may be seen from results presented in Table III that the corrugation force between a NaCl crystal and a tip of radius 2 Å amounts to 25% of the total van der Waals force $F(l, d)$ at a typical distance $\bar{d} = d - a$ equal to 2.5 Å. Note that in the continuum model used to describe the probe, the nucleus of the outermost atoms are located half an interatomic distance from the surface of the sphere. This means that when $\bar{d} = 2.5$ Å the real distance between the nucleus of the nearest atoms of the sample and of the probe are at about 3.5 Å. For the same crystal the results given in Table IV indicate that the corrugation force is weaker along the Na⁺ cation rows. In fact this behavior is due to the weak value of the in-crystal polarizability of Na⁺ (1.002 a.u.) and consequently of the strength coefficient C_{as} (cf. Table I). Such a modulation of the attractive force can be detected from the actual AFM which reaches a sensibility of 10^{-12} N.⁶ In the case of a MgO crystal, the atomic density in each plane (p) is greater than in NaCl, so that the corrugation force is smaller for same tip and same distance of nearest approach $\bar{d} = d - a$.

(iii) Figure 2 represents the whole attractive force be-

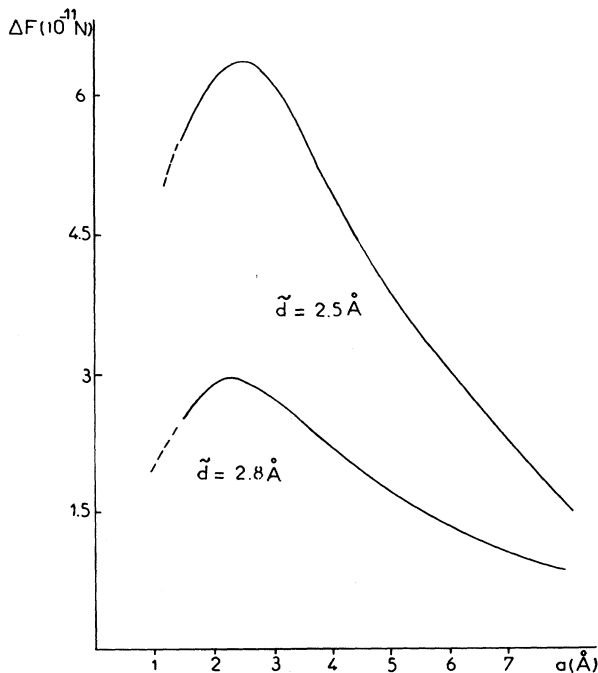


FIG. 4. The corrugation force experienced by a spherical probe as a function of its radius a : $\bar{d} = d - a$.

TABLE VII. The corrugation force ΔF experienced by a spherical probe as a function of the distance $\bar{d} = d - a$; ΔF is calculated for the (100) face of NaCl.

\bar{d} (Å)	$a = 2.5$ Å ΔF^a (10^{-11} N)	$a = 3$ Å ΔF (10^{-11} N)
2	25.7	14.8
2.5	4.81	6.38
3	1.92	1.59
3.5	0.53	0.49
4	0.17	0.14
4.5	0.054	0.049
5	0.02	0.016
5.5	0.006	0.006

^a $\Delta F = F(\text{Na}) - F(\text{Cl})$, where $F(\text{Na})$ and $F(\text{Cl})$ represent the force experienced by the probe above the sites Na and Cl, respectively.

tween a tip or radius equal to 2 Å and a (100) face of NaCl for two different distances \bar{d} and by scanning four primitive cells of the surface. When the distance \bar{d} increases from 2 to 2.5 Å, one remarks that expected corrugation decreases drastically. This behavior is consistent with the fast variation of the Bessel function $K_3(g[(d + pb)^2 - a]^{1/2})$ occurring in Eq. (30). Figure 3 represents the variation of the tip height \bar{d} for two different values of the van der Waals force between the probe and the (100) face of NaCl. One observes from Fig. 3(b) that for $F = 3.8 \times 10^{-10}$ N and $a = 2.5$ Å, \bar{d} varies from 2.7 to 2.92 Å. Note that for weak values of the distance ($\bar{d} \leq 2.5$ Å), the dispersion spatial effect due to the delocalized character of the response of the electrons moving in the probe should be introduced in the calculation of the van der Waals force.³⁶ In a first step we have neglected such nonlocal effects which, in a general way, slightly decrease the magnitude of the van der Waals interaction.²⁵

(iv) In order to discuss the influence of radius a of the probe on the AFM resolution we have plotted in Fig. 4 the corrugation magnitude $\Delta F(a)$ as a function of the radius a [$\Delta F(a) = F(\text{Cl}^-) - F(\text{Na}^+)$] for two distances \bar{d} . As expected the resolution decreases when the tip becomes too large. Moreover, it is important to note that the function $\Delta F(a)$ exhibits a maximum for a critical size $a_c \approx 2.6$ Å of the probe. This singular behavior may seem surprising. Indeed when the radius a decreases we could expect a better resolution. In fact, in this case, the total force decreases also as a^{-3} which explains the behavior of curves given in Fig. 4. Moreover, the results of Table VII exhibit the strong decrease of the corrugation force ΔF experienced by the probe for distances $\bar{d} > 3$ Å.

V. CONCLUSION

We have described a discrete model for calculating the van der Waals interaction between a real surface and a probe tip. In order to go beyond the continuum approximation introduced in previous papers, we have built a pairwise potential by taking into account all atoms in the solid. By working in the reciprocal lattice (g), this pro-

cedure allows us to isolate the corrugation part of the total force experienced by the tip: a small tip or a small protusion on a larger tip is needed to see atomic corrugations in the attractive mode. Moreover, in the case of NaCl, our model shows the existence of a critical size of the probe around the value $a \approx 2.6 \text{ \AA}$. The method described in Sec. III is not limited to fcc crystals but can be easily applied to more complicated symmetry (graphite, diamond, quartz, . . .). As it stands, our model could also be improved by including nonlocal effects²⁵ due to delocalized electrons moving in the tip and by introducing the repulsive force appearing at distances close to the

contact.³⁶ This last improvement will allow the study of repulsive mode used in AFM to image surfaces with very small atomic corrugations.

ACKNOWLEDGMENTS

The Laboratoire de Physique Moléculaire is "Unité associée au Centre National de la Recherche Scientifique No. 772." The Laboratoire d'Optique P. M. Duffieux is "Unité associée au Centre National de la Recherche Scientifique No. 214."

-
- ¹J. N. Israelachvili, *Intermolecular and Surfaces Forces* (Academic, New York, 1985), and references therein.
- ²H. C. Hamaker, *Physica* **4**, 1058 (1937).
- ³E. M. Lifshitz, *Zh. Eksp. Teor. Fiz.* **29**, 94 (1955). [*Sov. Phys.—JETP* **2**, 73 (1956)].
- ⁴I. E. Dzyloshinskii, E. M. Lifshitz, and L. P. Pitaevski, *Adv. Phys.* **10**, 165 (1961).
- ⁵G. Binning, C. F. Quate, and Ch. Gerber, *Phys. Rev. Lett.* **56**, 930 (1986).
- ⁶Y. Martin, C. C. Williams, and H. K. Wickramasinghe, *J. Appl. Phys.* **61**, 4723 (1987).
- ⁷Y. Martin and H. K. Wickramasinghe, *Appl. Phys. Lett.* **50**, 1455 (1987).
- ⁸D. W. Abraham, C. C. Williams, and H. K. Wickramasinghe, *Appl. Phys. Lett.* **5**, 1446 (1988).
- ⁹Y. Martin, D. Rugar, and H. K. Wickramasinghe, *Appl. Phys. Lett.* **52**, 2243 (1988).
- ¹⁰G. Binning, Ch. Gerber, E. Stoll, T. R. Albrecht, and C. F. Quate, *Europhys. Lett.* **3**, 1281 (1987).
- ¹¹O. Marti, B. Drake, and P. K. Hansma, *Appl. Phys. Lett.* **51**, 484 (1987).
- ¹²T. R. Albrecht and C. F. Quate, *J. Appl. Phys.* **62**, 2599 (1987).
- ¹³H. J. Mamin, E. Gantz, D. W. Abraham, R. E. Thomson, and J. Clarke, *Phys. Rev. B* **34**, 9015 (1986).
- ¹⁴J. M. Soler, A. M. Baro, and N. Garcia, *Phys. Rev. Lett.* **57**, 444 (1986).
- ¹⁵U. Durig, J. K. Gimzewski, and D. W. Pohl, *Phys. Rev. Lett.* **57**, 2403 (1986).
- ¹⁶J. J. Garcia, *Appl. Phys. Lett.* **53**, 1449 (1988).
- ¹⁷G. M. McClelland, R. Erlandsson, and S. Chiang, *Rev. Prog. Quantit. Nondestruct. Evaluation* **68**, 1307 (1988).
- ¹⁸J. Tersoff and D. R. Hamann, *Phys. Rev. Lett.* **50**, 199 (1983).
- ¹⁹W. A. Steele, *The Interaction of Gases with Solid Surfaces* (Pergamon, Oxford, 1974).
- ²⁰H. Hoinkes, *Rev. Mod. Phys.* **52**, 933 (1980).
- ²¹V. Celli, D. Eichenauer, A. Kaufhold, and J. P. Toennies, *J. Chem. Phys.* **83**, 2504 (1985).
- ²²G. Vidali, M. W. Cole, and J. R. Klein, *Phys. Rev. B* **28**, 3064 (1983).
- ²³G. Vidali and D. R. Frankl, *Phys. Rev. B* **27**, 2480 (1983).
- ²⁴C. Girard and C. Girardet, *J. Chem. Phys.* **86**, 6531 (1987).
- ²⁵C. Girard and C. Girardet, *Phys. Rev. B* **36**, 909 (1987).
- ²⁶T. Meichel, J. Suzanne, C. Girard, and C. Girardet, *Phys. Rev. B* **38**, 3781 (1988).
- ²⁷C. Girardet and C. Girard, *Surf. Sci.* **195**, 173 (1988).
- ²⁸C. Girard and C. Girardet, *Chem. Phys. Lett.* **138**, 83 (1987).
- ²⁹J. Mahanty and B. W. Ninham, *Dispersion Forces* (Academic, London, 1976).
- ³⁰C. Girard, *J. Chem. Phys.* **85**, 6750 (1986).
- ³¹A. M. Marvin and F. Toigo, *Phys. Rev. A* **25**, 782 (1982).
- ³²S. Maghezzi, C. Girard, and F. Hache (unpublished).
- ³³B. B. Dasgupta and R. Fuchs, *Phys. Rev. B* **24**, 554 (1981).
- ³⁴C. Girard, J. M. Vigoureux, and C. Girardet, *J. Chim. Phys.* **84**, 809 (1987).
- ³⁵P. W. Fowler and J. H. Hutson, *Surf. Sci.* **165**, 289 (1986).
- ³⁶C. Girard, S. Maghezzi, and D. Van Labeke (unpublished).